Electron-electron interaction and localization in d and f transition metals

D. van der Marel
Faculty of Applied Physics, Delft University of Technology, 2628-CJ Delft, The Netherlands

G. A. Sawatzky
Department of Applied Physics, University of Groningen, 9747-AG Groningen, The Netherlands
(Received 24 February 1987; revised manuscript received 27 October 1987)

We discuss, for the d and f transition metals, the competition between atomiclike electrostatic Coulomb and exchange interactions and loss of atomic characteristics in the solid through screening of f and d charge fluctuations and hybridization. We derive semiempirical relations describing these interactions for the $3d$, $4d$, $5d$, $4f$, and $5f$ elements in the environment of a metallic host. We then compare these to the hybridization widths, also semiempirically determined, and arrive at conclusions concerning the localization of the d or f electrons and the formation of magnetic moments. We show that some of the light actinides can exhibit negative U^{eff} behavior dependent on their valence in the solid. We argue that some d transition metals may belong to the same group if properly alloyed.

INTRODUCTION

During the last two decades it has become more and more customary among solid-state physicists to assume that the single-particle band picture is the correct starting point for studying the electronic structure of $3d$, $4d$, and $5d$ transition metals. The physics of the rare-earth metals, on the the other hand, is normally based on an atomic description of the f electrons, treating the f shell as a partly filled core shell. Rare-earth compounds exhibiting physical properties corresponding to noninteger occupation of the f shell are considered as exceptions and indicated as mixed-valence compounds. The field of actinide intermetallic compounds is rapidly growing and there is no consensus yet on how to treat the $5f$ shells of these elements. In this paper we discuss the electronic structure of the d and f valence electrons of transition-metal atoms embedded in a metallic host. We will not attempt to give a complete review of the literature on d and f transition metals; instead, we refer the reader to some review articles.[1-11]

One of the key features of a transition metal is the fact that the partly filled d or f shell is spatially localized around the nucleus. To illustrate the degree of spatial confinement, we plot in Fig. 1 the ratio of the f and d volumes to the Wigner-Seitz volume[12-14] $(r_l/r_{\text{WS}})^3$. We use published Hartree-Fock values for $\langle r_l^2 \rangle$ for the $3d$, $4d$, and $5d$ series, the $4f$ series,[15] and for the $5f$ series.[16-19] We see in Fig. 1 that all values are smaller than 1, indicating that the d and f wave functions are located well inside the Wigner-Seitz cell. We will see below the $(r_l/r_{\text{WS}})^3$ is a good approximation of the hybridization between localized states and conduction bands. Roughly speaking, the $4f$ shells of the lanthanides are more confined than the $5f$ shells of the actinides, which are again better shielded than the $3d$ shells, followed by the $4d$ and $5d$ shells. In this paper emphasis will be on transition elements embedded in a simple metallic host, such as Cu, Ag, Cd, or Zn. The only relevant hybridization in our discussion will be the hybridization with the host sp conduction bands, which we treat using the nearly-free-electron approximation. The hybridization matrix elements are given by Harrison,[20,21]

$$V_{kd}=\frac{1}{(N_a)^{1/2}}\frac{\hbar^2k^2}{m}\left[\frac{r_d}{r_{\text{WS}}}\right]^{3/2}Y_{2m}(\hat{k})\,, \tag{1}$$

$$V_{kf}=\frac{1}{(N_a)^{1/2}}\frac{\hbar^2k^2}{m}(kr_f)\left[\frac{r_f}{r_{\text{WS}}}\right]^{3/2}Y_{3m}(\hat{k})\,, \tag{2}$$

where N_a is the number of atoms.

The virtual-bound-state half-width at half maximum is given by

$$\Delta(\varepsilon)=\pi\,\text{Im}\sum_k (V_{kl})^2\delta(\varepsilon-\varepsilon_k)\,. \tag{3}$$

In what follows we will use $\Delta(\varepsilon_F)$ as a measure of hybridization of the localized state. From Eqs. (1)–(3) and using the standard expressions of free-electron theory for the density of state at the Fermi level, we arrive at

$$\Delta(\varepsilon_F)=\tfrac{3}{4}\varepsilon_F\left[\frac{r_d}{r_{\text{WS}}}\right]^3 Z \tag{4}$$

for d states, and

$$\Delta(\varepsilon_F)=\tfrac{3}{4}(r_fk_F)^2\varepsilon_F\left[\frac{r_f}{r_{\text{WS}}}\right]^3 Z \tag{5}$$

for f states.

Z is the number of electrons per host atom and ε_F is the Fermi energy of the host material. The Wigner-Seitz volume of the transition metal is assumed not to depend on the host material, i.e., we restrict our analysis to dilute alloys obeying Vegard's law, In Table I we accumulate the Δ's for the transition metals, using the Wigner-Seitz volumes of their elemental form and taking $\varepsilon_F=5.5$ eV,

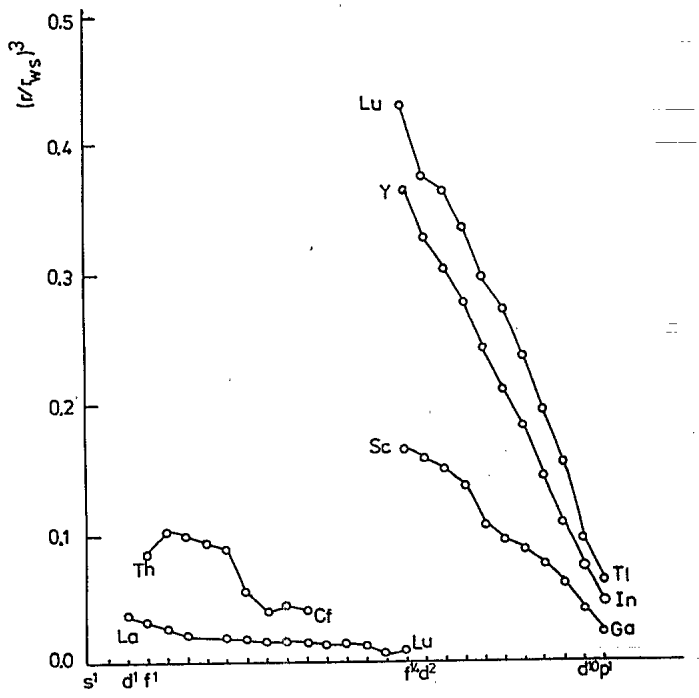

FIG. 1. Ratio of d and f shell volume to Wigner-Seitz volume of the transition elements.

which is typical for Ag and Au host materials. It is reassuring that the values for Δ so obtained agree reasonably well with experimentally determined values.[22–24] Differences may occur due to lattice strain effects and due to the fact that the conduction-band density of states in Eq. (3) may differ from the free-electron value of ε_F.

Apart from the size effect, the energies of the f and d electrons and their mutual interactions are extremely important for the understanding of the physical properties of these elements and their compounds. The important questions to be answered are: What are the energies involved in adding (removing) one or more electrons to (from) an atom in a given state, and what energies are involved in changing the electronic configuration within the d (f) shell without changing its polarity?

From the experimental point of view these questions correspond to: What are the x-ray photoemission spectroscopy (XPS) and ultraviolet photoemission spectroscopy (UPS) (one-electron removal), the Auger-electron spectroscopy (AES) CVV (two-electron removal), and the bremsstrahlung isochromat spectroscopy (BIS) (one-electron addition) spectra. The change in electronic configuration at equal polarity shows up as multiplet structure of the final states in the spectroscopies mentioned so far and in x-ray-absorption spectroscopy near-edge multiplet structures.

From the theoretical point of view the logical thing to do is to look at the Slater theory of atomic structure for the localized states, bearing in mind that the one-electron potentials may be totally different in the solid compared to the gas phase and also that the intrashell Coulomb interactions are screened by the conduction electrons. In the multiplet theory of the open-shell problem the energy of a state having n d(f) electrons and total orbit, spin, and seniority quantum numbers L, S, and λ is given by[25,26]

$$E(n,L,S,\lambda)=nI+\tfrac{1}{2}n(n-1)U_{\rm av}+U(n,L,S,\lambda)\ , \qquad (6)$$

where I is the one-electron potential, $U_{\rm av}$ is the multiplet-averaged Coulomb-exchange interaction energy, and $U(n,L,S,\lambda)$ is the multiplet splitting. For d electrons ($l=2$),

$$U_{\rm av}(dd)=F^0-\tfrac{2}{63}(F^2+F^4)=F^0-\frac{2}{4l+1}J(dd)\ . \qquad (7)$$

For f electrons ($l=3$),

$$U_{\rm av}(ff)=F^0-\tfrac{2}{27\,885}(286F^2+195F^4+250F^6)$$
$$=F^0-\frac{2}{4l+1}J(ff)\ . \qquad (8)$$

For later use it is convenient to introduce the exchange

TABLE I. Hybridization widths Δ of the valence d and f shells of the transition metals using Eqs. (4) and (5).

3d elements	Δ (eV)	4d elements	Δ (eV)	5d elements	Δ (eV)	4f elements	Δ (eV)	5f elements	Δ (eV)
Sc	0.71	Y	1.52	Lu	1.78	La	0.142	Ac	
Ti	0.65	Zr	1.35	Hf	1.56	Ce	0.077	Th	0.231
V	0.62	Nb	1.25	Ta	1.49	Pr	0.055	Pa	0.166
Cv	0.51	Mo	1.14	W	1.38	Nd	0.045	U	0.145
Mn	0.43	Tc	0.99	Re	1.22	Pm		Np	0.127
Fe	0.39	Ru	0.88	Os	1.13	Sm	0.031	Pu	0.102
Co	0.36	Rh	0.74	Ir	0.97	Eu	0.018	Am	0.071
Ni	0.31	Pd	0.59	Pt	0.89	Gd	0.023	Cm	0.070
Cu	0.25	Ag	0.44	Au	0.86	Tb	0.022	Bk	0.068
						Dy	0.019	Cf	0.066
						Ho	0.017		
						Er	0.016		
						Tm	0.014		
						Yb	0.009		
						Lu	0.009		

interactions $J(dd)$ and $J(ff)$ here, describing the intra-shell exchange attraction between parallel spins:

$$J(dd)=\tfrac{1}{14}(F^2+F^4)\ , \tag{9}$$

$$J(ff)=\tfrac{1}{6435}(286F^2+195F^4+250F^6)\ , \tag{10}$$

and the additional parameters describing the angular part of the multiplet splitting are

$$C(dd)=\tfrac{1}{14}(\tfrac{9}{7}F^2-\tfrac{5}{7}F^4)\ , \tag{11}$$

$$C(ff)=\tfrac{1}{6435}(286F^2+\tfrac{780}{11}F^4-\tfrac{1750}{11}F^6)\ . \tag{12}$$

The J's and C's are especially useful when describing the lowest state of an l^n multiplet. According to Hund's rule this is always the state with the highest possible spin quantum number. The energy expressions in terms of J and C, instead of F^2, F^4, and F^6, are very clear and F^0 and J are to be multiplied with simple combinatorial factors. We can express the Hund's-rule ground-state energies as

$$E_{\rm HR}(n)=\alpha_I(n)I+\alpha_{F^0}(n)F^0+\alpha_J(n)J+\alpha_C(n)C\ , \tag{13}$$

where the α's are given in Tables II and III. The physical meaning of F^0, J, and C is as follows:

$$F^0=\frac{1}{2l+1}\sum_{\substack{m,n\\ m<n}}\int d^3r_1\int d^3r_2\,|\,\Psi_{lm}(r_1)\,|^2 \times\frac{1}{r_{12}}\,|\,\Psi_{ln}(r_2)\,|^2\ , \tag{14}$$

which is the average value of the static Coulomb repulsion between the charge distributions corresponding to two electrons in the same shell,

$$J=\frac{1}{2l+1}\sum_{\substack{m,n\\ m<n}}\int d^3r_1\int d^3r_2\left[\Psi_{lm}(r_1)\Psi_{ln}(r_1)\frac{1}{r_{12}} \times\Psi_{lm}(r_2)\Psi_{ln}(r_2)\right]\ , \tag{15}$$

which is the average value of the exchange integral of two electrons in the same shell.[27] At incomplete filling (in this context "complete" means either full or half-filled) there are contributions to the total energy due to the nonspherical shape of the charge distribution, which is expressed by C. This parameter contains all multipole contributions of both Coulomb and exchange integrals. Note that the coefficients α_c show particle-hole symmetry.

Also given in these tables are the energy expressions for the Hubbard U,

$$U^{\rm eff}=E_{\rm HR}(n+1)+E_{\rm HR}(n-1)-2E_{\rm HR}(n)\ , \tag{16}$$

which is the energy involved in the reaction

$$2f^n_{\rm HR}\rightarrow f^{n+1}_{\rm HR}+f^{n-1}_{\rm HR}\ .$$

This corresponds to the gap between the valence photoemission and BIS spectra of the d or f states. For d and f states the C's are about half the J's and the latter vary from 0.8 to 1.4 eV for Sc up to Lu, and from 0.9 to 1.4 eV for La up to Yb. We can see from Tables II and III that the Hubbard U for the half-filled shell is always $(2l+1)J$ larger then for the other occupation numbers, apart from contributions of the C's. This amounts to 4–8 eV for the $3d$ and $4f$ elements. Now the parameters in Tables II and III describe the situation in an atom with an open d or f shell without any other charges in the system. Even in the case of gas-phase atoms there are valence electrons that interact among themselves and with the open d or f shell. This leads to further multiplet splitting of the states and to extra configuration interactions. In the solid this situation is extremely complicated due to the virtually infinite number of particles involved. A potentially successful approach to this problem is to make a formal separation between the highly correlated f and d

TABLE II. Parameters determining the energies of the Hund's rule ground states in LS coupling for all d occupations and the expression for the d-d gap.

State	α_I	α_{F^0}	α_J	α_c	$U^{\rm eff}$
$d^0(^1S)$	0	0	0	0	
$d^1(^2D)$	1	0	0	0	F^0-J-C
$d^2(^3F)$	2	1	−1	−1	F^0-J+C
$d^3(^4F)$	3	3	−3	−1	F^0-J+C
$d^4(^5D)$	4	6	−6	0	F^0-J-C
$d^5(^6S)$	5	10	−10	0	F^0+4J
$d^6(^5D)$	6	15	−10	0	F^0-J-C
$d^7(^4F)$	7	21	−11	−1	F^0-J+C
$d^8(^3F)$	8	28	−13	−1	F^0-J+C
$d^9(^2D)$	9	36	−16	0	F^0-J-C
$d^{10}(^1S)$	10	45	−20	0	

TABLE III. Parameters determining the energies of the Hund's rule ground states in LS coupling for all f occupations and the expression for the f-f gap.

State	α_I	α_{F^0}	α_J	α_C	$U^{\rm eff}$
$F^0(^1S)$	0	0	0	0	
$F^1(^2F)$	1	0	0	0	$F^0-J-3/2C$
$F^2(^3H)$	2	1	−1	$-\frac{3}{2}$	$F^0-J-1/2C$
$F^3(^4I)$	3	3	−3	$-\frac{7}{2}$	F^0-J+2C
$F^4(^5I)$	4	6	−6	$-\frac{7}{2}$	F^0-J+2C
$F^5(^6H)$	5	10	−10	$-\frac{3}{2}$	$F^0-J-1/2C$
$F^6(^7F)$	6	15	−15	0	$F^0-J-3/2C$
$F^7(^8S)$	7	21	−21	0	F^0+6J
$F^8(^7F)$	8	28	−21	0	$F^0-J-3/2C$
$F^9(^6H)$	9	36	−22	$-\frac{3}{2}$	$F^0-J-1/2C$
$F^{10}(^5I)$	10	45	−24	$-\frac{7}{2}$	F^0-J+2C
$F^{11}(^4I)$	11	55	−27	$-\frac{7}{2}$	F^0-J+2C
$F^{12}(^3H)$	12	66	−31	$-\frac{3}{2}$	$F^0-J-1/2C$
$F^{13}(^2F)$	13	78	−36	0	$F^0-J-3/2C$
$F^{14}(^1S)$	14	91	−42	0	

states and the valence electrons (which include the $5d$ and $6d$ states in case of the lanthanides and the actinides), that fall into wide bands due to strong hybridization. The latter can then be treated in terms of local-density theory, whereas the former are treated as a quasiatomic open-shell system, always allowing the conduction states to relax to each new polarity state of the d or f "cores." Herbst *et al.* performed such calculations for the lanthanides and the actinides.[28–31] Dederichs *et al.* used a very promising and potentially powerful *ab initio* formalism to treat Ce.[32]

Herring[4] introduced a simple method to estimate the effect of screening on U^{eff} by replacing the reaction of Eq. (16) with

$$2d^n s \rightarrow d^{n+1} + d^{n-1} s^2 ,$$

and similar expressions for the f shell systems. The philosophy is that in a metallic system the screening of a localized electron or hole is always such that charge neutrality is maintained.[33] The assumption is that this happens at the impurity site, which is not exact, but quite reasonable for many cases. The energies involved in the fully screened reaction can now be obtained from the gas-phase optical data involving the transitions $d^n \rightarrow d^{n-1} s$, always taking the Hund's-rule ground states for each d occupation. The charge-neutrality argument also shows that F^2, F^4, and F^6, or in other words, J and C, must be quite insensitive to placing the atom in a solid, as the splittings within a given d^n multiplet do not involve a different polarity of the atom.

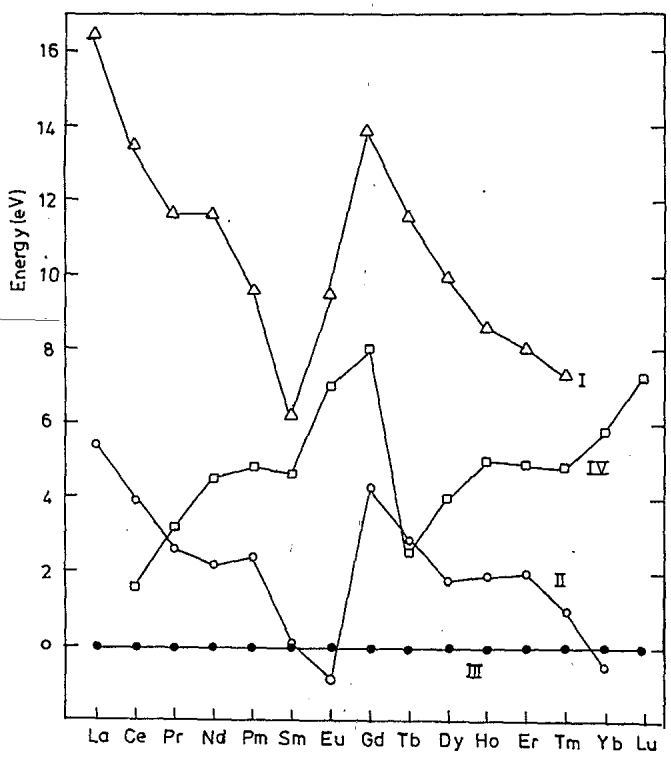

FIG. 2. Energies of rare-earth Hund's-rule ground states of monovalent (I), divalent (II), trivalent (III) and tetravalent (IV) rare earths relative to the trivalent state using the interpolation method discussed in the text.

DISCUSSION

We discuss F^0, J, and C obtained from two different sources. The first source is Mann's[34] compilation of single-particle energies and Coulomb integrals for the elements based on the Hartree-Fock method. These parameters correspond to the static configuration of neutral isolated atoms. Therefore, no screening contribution to the energy of a charged state is included. The second source is empirical optical data of the atomic energy levels. Using Herring's technique, which we explained in the Introduction, we get reasonable estimates of the effective parameters F^0, J, and C including the screening contribution of a metallic environment. In Table IV we list interpolation formula for these parameters as a function of atomic number. The empirical values of J and C are based on gas-phase multiplet splittings of the $3d$ series, on Racah parameters fitted to lanthanide-compound optical spectra,[9] and on Racah parameters fitted to optical[33,36] and photoemission multiplet[37–39] spectra of the actinide oxides. We see from the table that the measured J's and C's are always some 20–30 % reduced compared to the Hartree-Fock values, whereas the reduction of the F^0's is much stronger. We will discuss below how the

TABLE IV. Interpolation formulas for F^0, J, and C as a function of atomic number Z.

Row	Parameter	Hartree-Fock	Empirical
$3d$	F^0	$15.31+1.50(Z-21)$	$1.5+0.21(Z-21)$
	J	$0.81+0.080(Z-21)$	$0.59+0.075(Z-21)$
	C	$0.52J$	$0.51J$
$4d$	J	$0.59+0.056(Z-39)$	
	C	$0.50J$	
$5d$	J	$0.60+0.053(Z-71)$	
	C	$0.52J$	
$4f$	F^0	$23.8+0.93(Z-57)$	$6.7+0.033(Z-57)$
	J	$0.90+0.036Z-57)$	$0.69+0.014(Z-57)$
	C	$0.50J$	$0.45J$
$5f$	J	$0.66+0.035(Z-89)$	$0.33+0.070(Z-89)$
	C	$0.41J$	$0.41J$

empirical estimates of F^0 were obtained.

The most clearcut case for this discussion is the lanthanide row. We interpolate energies of the lowest Hund's-rule state for various occupations of the f shell and compare those with the XPS and BIS data of Lang *et al.*[40,41] We will do this by assuming a linear dependence of I and F^0 on atomic number Z, using Table IV for J and C and neglecting spin-orbit interaction.

The best parametrization that we obtained was

$$I = 5.4 - 7.071(Z-57) \text{ eV} ,$$
$$F^0 = 6.68 + 0.0333(Z-57) \text{ eV} . \quad (17)$$

In Fig. 2 we plotted the energies of the monovalent, divalent, and trivalent Hund's-rule ground states of the lanthanides using Eqs. (17) and Tables II and IV. Curve II has the same shape as the calculated energies of the $f^n d^1 s^2$ configurations of Nugent and van der Sluis.[42] Several trends are quite clear in Fig. 2: Eu and Yb are divalent, and Sm is close to becoming divalent and is therefore a likely candidate for mixed-valence behavior. If anything, Ce will become tetravalent. Good candidates to do mixed-valent chemistry on are, therefore, Sm, Eu, Tm, Yb, and Ce. This is in good agreement with experimental observation.[6]

In Fig. 3 we give the energy positions of the BIS and XPS Hunds'-rule levels of Lang *et al.*,[40] together with the interpolation values using Eqs. (17) and Table IV, taking the ground-state energies from Fig. 4. We see, that the 25 experimental peak positions are surprisingly well reproduced in our four-parameter fit. We also indicate the theoretical values of Herbst *et al.*,[30] which are in good agreement with the experimental values apart from a systematic shift of several tenths of an eV towards higher binding energy. In cerium Lang *et al.* observed a state very close to E_F. This feature has been explained convincingly by Günnarsson and Schönhammer[43] using a $1/N_f$ expansion. They showed that hybridization of the f shell with the valence bands results in a self-energy shift of the photoemission features. The input parameters for the f^0-f^1 separation, ε_f, and the f^2-f^1 separation, $\varepsilon_f + U^{\text{eff}}$, that they used for fitting their theory to the experimental spectra (this is different from the calculated peak positions) are also indicated in Fig. 3 and are close to our interpolation values.

Finally, we compare in Table V the U^{eff} from Lang *et al.* with the values from our interpolation and with the values obtained from optical data[44] using the method outlined in the Introduction as far as the necessary data were available. From Table V we see that both the interpolation method and the optical data predict the observed U^{eff} within a few tenths of an eV. The optical data underestimate U^{eff} by about 0.35 eV on the average.

The situation in the $3d$ series is different from the $4f$ series. The U^{eff} is much smaller in this case, so that interconfigurational mixing in the ground state can be

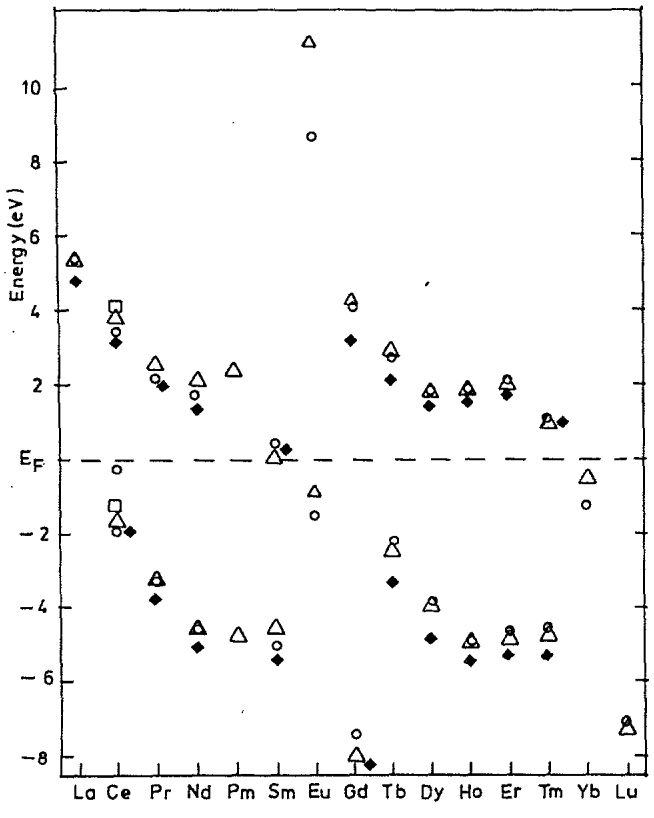

FIG. 3. BIS and XPS binding energies of rare-earth f states closest to the Fermi level. ○, experimental work by Lang *et al.* (Ref. 40); △, results from the four-parameter interpolation; □, theoretical results by Günnarsson and Schönhammer (Ref. 43); ◆, theoretical results by Herbst (Ref. 30).

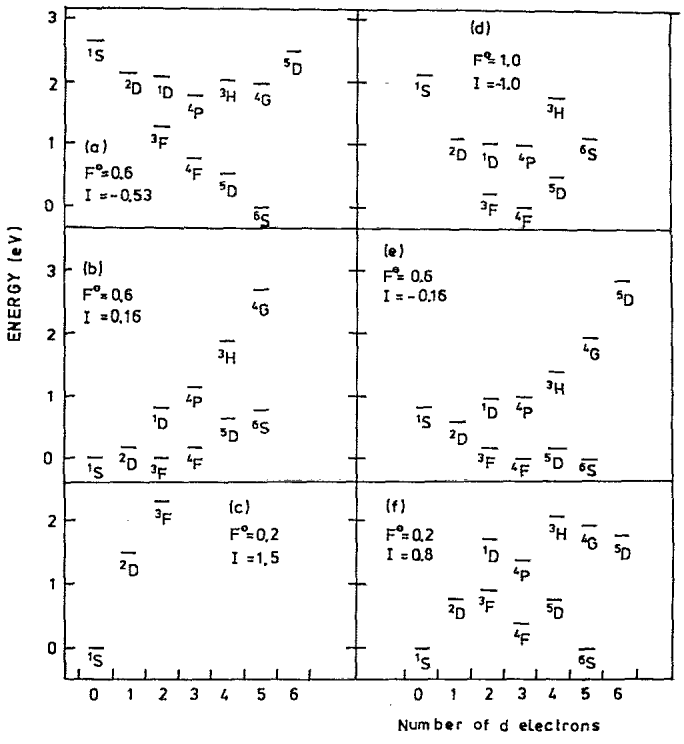

FIG. 4. Calculated energy positions of lowest and first excited states as a function of d occupation for indicated parameter values of $F^0$and I and taking $F^2=5.2$ eV and $F^4=3.2$ eV.

TABLE V. U^{eff} (eV) corresponding to the indicated reaction and elements.

Element	Reaction	Optical	XPS and BIS	Interpolation
Ce^{3+}	$2(f^1ds^2)\rightarrow f^2s^2+d^2s^2$	5.1	5.4	5.5
Pr^{3+}	$2(f^2ds^2)\rightarrow f^3s^2+f^1d^2s^2$	5.3	5.5	5.8
Nd^{3+}	$2(f^3ds^2)\rightarrow f^4s^2+f^2d^2s^2$	6.0	6.4	6.7
Sm^{3+}	$2(f^5ds^2)\rightarrow f^6s^2+f^4d^2s^2$		5.5	4.7
Sm^{2+}	$2(f^6s^2)\rightarrow f^7s+f^5ds^2$	5.1		
Tm^{3+}	$2(f^{12}ds^2)\rightarrow f^{13}s^2+f^{11}d^2s^2$		5.7	5.8
Tm^{2+}	$2(f^{13}s^2)\rightarrow f^{14}s+f^{12}ds^2$	5.4		

considerable. Consequently, the extraction of F^0, J, and C from UPS, BIS, and AES data[45,50] is often a difficult task. On the other hand, the gas-phase optical data cover a relatively wide range of d occupations for most $3d$ elements. The available data are collected in Table VI. From this table we obtain values which are some 20 eV below the bare Hartree-Fock values (see Table IV), as in the lanthanides. We see that the value of F^0 in Mn is different for both methods, but note that the valence is also different in both cases.

The degree of agreement for Cr and Ni is comparable to what we found in the lanthanides. The optically determined values for F^0 in Sc, Ti, and V are quite high (1–2 eV), but as in the case of Mn the valence of these elements is different in the solid from that in the gas phase. As they are probably divalent or even trivalent, the screening can be somewhat larger than in, for example, monovalent Cr, so that the screened F^0 value is probably between 0 and 1 eV. If so, this would lead to negative values for U^{eff} as has been mentioned earlier by de Boer *et al.* in connection with their Auger analysis.[52]

To show what will happen in such cases, we have drawn in Fig. 4 energy-level diagrams of the Hund's-rule ground states and first-excited states as a function of occupation for some values of F^0 and I. We used $J=0.6$ eV and $C=0.31$ eV everywhere. Figure 4(a) corresponds roughly to Cr impurities. The d^4 state is close to the d^5 state, so that the ground state is of mixed d^5d^4 character. In view of this fact it is surprising that no clear features are observed close to the Fermi level, as one would expect if the ground state were purely d^4 or if a many-body resonance would build up at the Fermi level.[2] This paradox strongly resembles the paradox *Ag*Mn,[46] where we found a minority peak of a 2.1 eV from E_F having a half-width at half maximum (HWHM) of 1.2 eV. Andrews *et al.*[45] found the majority peak of Cr in Ar at 0.87 eV binding energy having a half-width of 0.28 eV. In both cases the ratio of half-width to peak position is in the range of $\frac{1}{2}$, indicating strong fluctuations between d^5 and d^6 in the case of *Au*Cr. Nevertheless, the spectral features are those of a pure d^5 state.

Figure 4(b) corresponds to Ti. Note that, although the single-particle potential I is repulsive, a d^2-state can still be favored due to the multiplet splitting. If F^0 gets smaller then J, we get a situation as in Fig. 4(f), where charge fluctuations take place involving more than two electrons. We must not forget, however, that the screening mechanism becomes very nonlinear if an atom has already lost all its screening electrons. Addition of an extra negative charge can no longer be compensated within the same unit cell, and the corresponding state will be several eV higher in energy then what is to be expected from linear-response theory. For Ti this would mean that states having more than four d electrons are no longer fully screened. In V the d^5 state is still possible and this means that the quite extreme situation of Fig. 4(f) could, in principle, occur in certain V alloys. Figure 4(d) or Fig. 4(e) is probably closer to *Au*V.

The $4d$ and $5d$ elements normally do not form magnetic moments, although there are exceptions. To our

TABLE VI. U^{eff} from various sources for the indicated reactions and the resulting F^0 value.

Element	Reaction	U^{eff} [a]	F^0 atomic	F^0 in solid[b]
Sc	$2(d^2s)\rightarrow ds^2+d^3$	1.05	1.27	
Ti	$2(d^3s)\rightarrow d^2s^2+d^4$	1.93	2.21	
V	$2(d^4s)\rightarrow d^3s^2+d^5$	1.34	2.36	
Cr	$2(d^5s)\rightarrow d^4s^2+d^6$	4.62	0.94	
Mn	$2(d^6s)\rightarrow d^5s^2+d^7$	1.31	2.75	
Mn	$2(d^5s^2)\rightarrow d^4(s^2p)+d^6s$			1.0
Fe	$2(d^7s)\rightarrow d^6s^2+d^8$	1.83	2.35	
Co	$2(d^8s)\rightarrow d^7s^2+d^9$	2.22	2.68	
Ni	$2(d^9s)\rightarrow d^8s^2+d^{10}$	1.61	3.21	3.9
Cu				5.9

[a]Reference 51.
[b]References 46–49.

knowledge there are no UPS and BIS data available from which U^{eff} values can be extracted. We therefore restrict the discussion to U^{eff} from optical data. These are collected in Table VII. We also indicated "F^0" estimates, using J's and C's that were taken to be 80% of the values of Table IV, however, without incorporating spin-orbit coupling. We see that although the Hartree-Fock values of F^0 are several eV lower than in the $3d$ series, the screened F^0 values stay at a lower limit of 1–2 eV, with the exception of Ta, where we find a negative Hubbard U. Nevertheless, the F^0 values could be still smaller in a metallic host due to the higher density of the conduction electrons. With the exception of Mo^+, Tc^{2+}, Re^{2+}, and W^+ we expect a small Hubbard U. The possibility of a negative U^{eff} is intriguing and we expect this to occur for elements having a d^1, d^4, d^6, or d^9 configuration, as we have already discussed for the $3d$ elements.

In the compounds of U, Np, Pu, and Am the actinide atoms possess magnetic moments of $(1-3)\mu_B$.[53] These moments are of mixed spin-orbital nature, the orbitular part not being quenched completely in the crystal fields. Well-developed moments exist especially in systems having interactinidic spacings of more than 3.5 Å.[54] Pure U, Np, and Pu form rather wide f bands and do not show magnetic ordering. Their effective intra-atomic interactions are known to be small due to screening,[55–57,31] although the exchange splittings of the atoms are comparable to those of the $3d$ metals. The f bands become very narrow, however, in compounds with large interactinidic distances.[58] The empirical C and J values of the actinides lie some 30% below those of the lanthanides. The spin-orbit parameter ranges from 0.23 to 0.40 eV from uranium to berkelium,[37] which is some 65% larger then the corresponding parameter in the chemically equivalent lanthanides.[9,59] In Table VIII we list the levels of the different f occupations of the neutral gas-phase actinides determined from optical data, always taking the lowest levels. In parentheses we give the assignments of the levels.[44] From this table we can derive U^{eff}, as in the preceding sections. Very significant are the many different crossing levels in U, Pa, and Np. As a consequence, we can define three different U^{eff} values for uranium dependent on its valence. Johansson arrived at a U^{eff} of 2.3 eV for uranium, which was based on the trivalent configuration,[56] but he did not mention the other valences. As uranium metal has two f electrons, the tetravalent U^{eff} is probably more important. In Table IX we list the U^{eff} values derived from Table VIII for the various valences that are possible.

As the single-electron potentials in the solid may differ significantly from those in the gas phase, the valence of the atoms can be different as well. To make clear what this implies in the light actinides, we have plotted in Fig. 5 the values of Table VIII for the different f occupations, while adding a single-electron potential to them, i.e., energy that depends linearly on the f occupation. This potential was chosen such that uranium ends up having ~ 2 electrons on the average, Np ~ 3 electrons, and Pa ~ 1.5 electrons. Of course, such choices are arbitrary and the value of the single-electron potential will depend on the electronegativity of the element(s) the actinide atom is (are) alloyed with. Figure 5 and Table IX show a feature that is probably crucial in the physics and chemistry of the light actinides. The negative U^{eff} causes nonstatistical charge fluctuations of two or even three electrons in the f shell. Especially if the f bands are narrow, this must give rise to peculiar and new phenomena. We believe that this may be a crucial feature of the actinide-based heavy-fermion systems.[60]

Finally, we will discuss the d and f transition metals using a plot of their Hubbard U against Δ (see Table I) which is sensitive to the degree of spatial confinement.

In Fig. 6 we display the positions of the pure metallic elements in such a plot. The U^{eff} values are the values of Tables V, VI, VII, and IX. Valences are also indicated; U^{eff} can easily be calculated for other valences using Tables II and III and the relations for F^0, J, and C in the hosts. The solid curves are the curves $U^{\text{eff}}=2\Delta$ and $U^{\text{eff}}=-2\Delta$. They divide the plane into three parts, where Δ is appropriate for a Ag or Au host.

Region I contains impurity atoms that obey Hund's rule and that couple weakly to the conduction bands. In these systems the valence of the atoms fluctuates between two values or it is fixed. Due to the large U^{eff} and the localized nature of the electrons, fluctuations involving

TABLE VII. U^{eff} (eV) from the indicated reactions using optical data (Ref. 51), the resulting F^0, and the F^0 from Mann's tables (Ref. 34).

Element	Reaction	U^{eff}	F^0	F^{0a}
Y	$2d^2s \rightarrow d^1s^2+d^3$	0.8	1.0	10.23
Zr	$2d^3s \rightarrow d^2s^2+d^4$	1.5	1.8	11.64
Nb	$2d^4s \rightarrow d^3s^2+d^5$	1.5	2.3	11.96
Mo	$2d^5s \rightarrow d^4s^2+d^6$	4.6	2.2	13.14
Ru	$2d^7s \rightarrow d^6s^2+d^8$	2.0	2.4	15.26
Rh	$2d^8s \rightarrow d^7s^2+d^9$	2.0	2.4	16.26
Pd	$2d^9s \rightarrow d^8s^2+d^{10}$	1.5	2.6	16.36
Ta	$2d^4s \rightarrow d^3s^2+d^5$	−1.0	−0.2	12.10
Ir	$2d^8s \rightarrow d^7s^2+d^9$	1.6	2.0	15.22
Pt	$2d^9s \rightarrow d^8s^2+d^{10}$	0.9	2.0	15.36

[a]Reference 34.

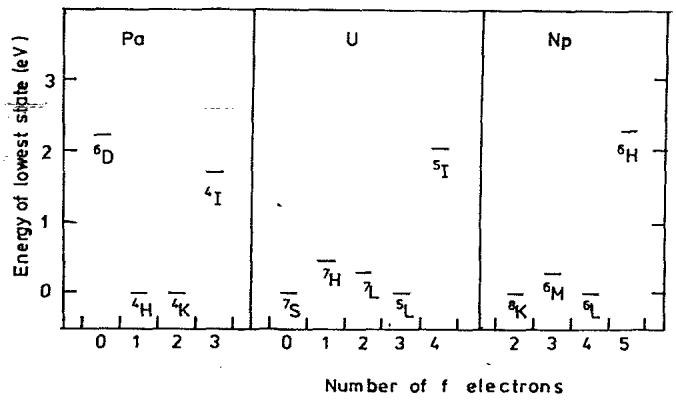

FIG. 5. Energy positions of lowest states as a function of f occupancy of U, Pa, and Np using Table VIII and adding an extra single-particle potential.

TABLE VIII. Energies (eV) of the indicated configurations using optical data (Ref. 44).

Element	f^0	f^1	f^2	f^3	f^4	f^5	f^6	f^7
Th	0.00 (d^2s^2)	0.97 (fds^2)	3.47 (f^2s^2)					
Pa	2.73 (d^4s)	0.25 (fd^2s^2)	0.00 (f^2ds^2)	1.42 (f^3s^2)				
U	3.47 (d^5s)	2.73 (fd^4s)	1.43 ($f^2d^2s^2$)	0.00 (f^3ds^2)	0.87 (f^4s^2)			
Np			4.34 (f^2d^4s)	2.42 ($f^3d^2s^2$)	0.00 (f^4ds^2)	0.12 (f^5s^2)		
Pu					4.47 ($f^4d^2s^2$)	0.78 (f^5ds^2)	0.00 (f^6s^2)	
Am						6.94 ($f^5d^2s^2$)	2.11 (f^6ds^2)	0.00 (f^7s^2)

more than two valences are suppressed, which usually results in magnetic-moment formation and the occurrence of the Kondo effect. It is not possible to predict the Kondo temperatures from this figure alone, as one needs to know the localized energy levels relative to the Fermi energy as well. We see from Fig. 6 that the rare-earth elements and most $3d$ elements as well as the actinides are in this region. In a few cases there is a large volume collapse from a high-temperature phase to a low-temperature phase [Pu (Ref. 7), Ce (Ref. 10), and Sm compounds (Refs. 11 and 61)], which has been interpreted as a Mott-Hubbard transition[55–57,18] involving localization of the f electrons. An alternative interpretation has been given for the Ce case,[62] where the phase transition is between two states having different Kondo temperatures. At the transition temperature the system collapses from a phase with a low Kondo temperature ($T > T_K = 55$ K) to a phase with a high Kondo temperature ($T < T_K = 766$ K).

Region II contains the elements for which the intrashell interactions form a relatively small perturbation to the impurity ground state. The Kondo effect does not occur for systems in this class, as the formation of local moments is prohibited by the strong valence fluctuations. Interestingly, Ta^+ and U^{4+} impurities fall in the negative-U^{eff} region. However, as they are located in Region II, it is not clear to us whether this will also affect the physical properties. At least the charge-fluctuation propagator $C^0(q,\omega)$ is enhanced with a factor $[1 + U^{\text{eff}}C^0(q,\omega)]^{-1}$ for negative-U^{eff} materials. An unstability is expected for $U^{\text{eff}}C^0(q,0) = -1$, resulting in a charge-density wave. In this context it is worth mentioning that two independent types of uranium atoms have been claimed in α-uranium.[63]

Region III is a very special class: A proper name would be "double-valence-fluctuation" systems. This term has been coined by Hirsch and Scalapino,[64] who discussed for d electrons the parameter regime where the on-site repulsion can be overcome by excitonic screening. In their case this involves screening by d electrons which are in the same shell as the conduction electrons, but which belong to a different representation of the point group. This differs from the present discussion, where the screening electrons are not in the same shell. The ground state of such impurities would be a mixture of f^{N-1} and f^{N+1} states, while f^N would be relatively unimportant (N is the *average* occupation of the f shell). The only candidates for this region are Np^{4+} and U^{5+}. In an earlier paper we discussed the possibility of odd-parity pairing of conduction electrons induced by the negative U^{eff} of the localized f electrons at the uranium sites in a fictitious ordered uranium compound.[65]

We want to emphasize that the light actinides have a special position in the U^{eff}-versus-Δ plot, in that they are

TABLE IX. U^{eff} (eV) for the actinides for several valences and corresponding reactions using optical data (Ref. 44).

Element	Valence	Reaction	U^{eff} (eV)
Th	III	$2fds^2 \rightarrow f^2s^2 + d^2s^2$	1.53
Pa	III	$2f^2ds^2 \rightarrow f^3s^2 + fd^2s^2$	1.67
Pa	IV	$2fd^2s^2 \rightarrow f^2ds^2 + d^4s$	2.23
U	III	$2f^3ds^2 \rightarrow f^4s^2 + f^2d^2s^2$	2.30
U	IV	$2f^2d^2s^2 \rightarrow f^3ds^2 + fd^4s$	−0.13
U	V	$2fd^4s \rightarrow f^2d^2s^2 + d^5s$	−0.56
Np	III	$2f^4ds^2 \rightarrow f^5s^2 + f^3d^2s^2$	2.64
Np	IV	$2f^3d^2s^2 \rightarrow f^4ds^2 + f^2d^4s$	−0.50
Pu	III	$2f^5ds^2 \rightarrow f^6s^2 + f^4d^2s^2$	2.91
Am	III	$2f^6ds^2 \rightarrow f^7s^2 + f^5d^2s^2$	2.72

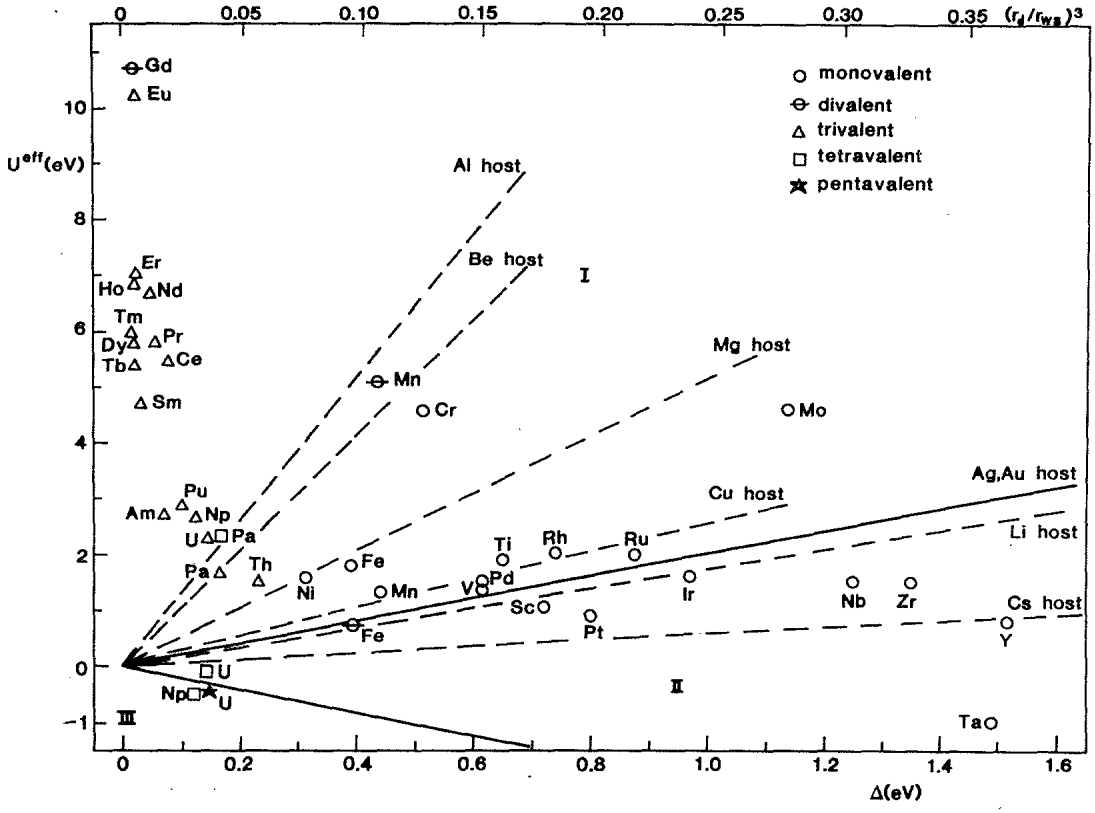

FIG. 6. Plot of U^{eff} against Δ for the transition metals. The assumed valences are indicated.

localized, but have a negative U^{eff}. We obtained this result using the same method as Johansson,[55–57] but we extended the method to the tetratravalent and pentavalent states. As the number of $5f$ electrons per uranium atom in UPt_3, URu_2, Si_2, and UBe_{13} lies between 2 and 3,[66,60] a situation close to that given in Fig. 5(b) may exist.

So far we have been discussing transition metals embedded in Au and Ag host materials. To point out what has to be expected in other hosts, we have drawn the dashed lines in Fig. 6 for several host materials. We used Eq. (4) for the d transition metals to plot U^{eff} against $(r_d/r_{\text{WS}})^2$ (indicated along the upper horizontal axis of Fig. 6). It is not possible to put the d- and f-shell materials in a single plot now, in view of the difference between Eqs. (4) and (5), so this part of the discussion is restricted to the d transition metals only. The dividing lines between regions I and II are now given by

$$U^{\text{eff}}/\tfrac{3}{2}\varepsilon_F Z = (r_d/r_{\text{WS}})^3 ,$$

and are indicated for Al, Be, Mg, Cu, Ag, Au, Li, and Cs. Values for $(\varepsilon_F Z)$ of any simple metallic host can be found in elementary textbooks on solid-state physics. The corresponding dividing line in our plot will then indicate whether an embedded transition-metal atom will exhibit local moment behavior. For example, we expect Mo^+ to have a well-developed d^5 local moment in Cu, Ag, Au and the alkali metals. On the other hand, if the atom were divalent, we expect Mo to have a U^{eff} of about 0.1 eV (using Tables II, IV, and VII), which would be well inside region II for all these host materials. Recently, it has been proved experimentally that Mo shows strong local magnetism in a Cs host.[67] This indicated that Mo should be regarded as monovalent in an alkali host and has a $4d^5$ configuration.

Another nice example is Mn in Al, which is at the delocalized side of the dividing line in our plot. Therefore, we expect it to exhibit no clear local-moment behavior, which is indeed a well-established fact.[68,69] Instead the magnetic susceptibility shows enhanced Pauli paramagnetism and a negative quadratic curvature is observed in the low-temperature resistivity with a scaling temperature of 900 K. These observations have been successfully interpreted in terms of localized spin fluctuations.[68–70] Divalent iron is in our plot at the border of being localized in Ag, Au, and Li hosts, whereas it is well localized for a Cs host. Again this agrees well with Riegel's results, who found local-moment behavior with a d^6 configuration for Fe in Cs, Rb, and K and instable behavior for Fe in Li.[71] From our plot we conclude that Pd, Rh, and Ru are unstable in Cu, but can form stable moments in the alakli metals.

CONCLUSIONS

From a quantitative comparison of Coulomb and exchange interactions to realistic estimates of hybridization widths of d and f transition metals in various host materials, it is possible to predict local-moment behavior, valence instabilities, and double-valence fluctuations. The last is a new class of materials and we predict such behavior for U and Np alloys.

ACKNOWLEDGMENTS

This investigation was supported in part by the Netherlands Foundation for Chemical Research (SON) and the Netherlands Foundation for Physical Research (FOM) with financial aid from the Netherlands Organization for the Advancement of Pure Research (ZWO).

[1]M. D. Daybell and W. A. Steyert, Rev. Mod. Phys. **40**, 380 (1968).
[2]G. Grüner and A. Zawadowski, Rep. Progr. Phys. **37**, 1497 (1974).
[3]N. Andrei, K. Furuya, and J. M. Löwenstein, Rev. Mod. Phys. **55**, 331 (1981).
[4]C. Herring, in *Magnetism,* edited by T. Rado and H. Suhl (Academic, New York, 1964), Vol. IV.
[5]A. J. Heeger, in *Solid State Physics,* edited by F. Seitz and D. Turnbull (Academic, New York, 1969), Vol. 23, p. 283.
[6]*Valence Instabilities and Related Narrow-Band Phenomena,* edited by R. D. Parks (Plenum, New York, 1977).
[7]*Structure and Bonding,* edited by L. Manes (Springer, Berlin, 1985), Vol. 59/60.
[8]*The Actinides, Electronic Structure and Related Properties,* edited by A. J. Freeman and J. B. Darby (Academic, New York, 1974), Pts. I and II.
[9]G. H. Dieke, in *Spectra and Energy Levels of Rare Earth Ions in Crystals,* edited by H. M. Crosswhite (Wiley, New York, 1968).
[10]D. C. Koskenmaki and K. A. Gschneider, in *Handbook on the Physics and Chemistry of the Rare Earths,* edited by K. A. Gschneider and L. Eyring (North-Holland, Amsterdam, 1978), Vol. I, Chap. 4.
[11]C. M. Varma, Rev. Mod. Phys. **48**, 219 (1976).
[12]N. W. Ashcroft and N. D. Mermin, *Solid State Physics* (Holt, Rinehart and Winston, New York, 1976), p. 1.
[13]*The Handbook of Chemistry and Physics,* 56th ed., edited by C. Weast (Chemical Rubber Co., Cleveland, 1975), p. B-237.
[14]L. Manes and U. Benedict, in *Structure and Bonding,* Ref. 7, p. 80.
[15]C. F. Fischer, *The Hartree-Fock Method for Atoms* (Wiley, New York, 1977).
[16]D. Liberman, J. T. Waber, and D. T. Cromer, Phys. Rev. **137**, A27 (1965).
[17]J. P. Desclaux, At. Data Nucl. Data Tables, **12**, 310 (1973).
[18]J. M. Fournier and L. Manes, in *Structure and Bonding,* Ref. 7. p. 3.
[19]W. Harrison, Phys. Rev. B **29**, 2917 (1984).
[20]W. Harrison, Phys. Rev. B **28**, 550 (1983).
[21]W. Harrison, *Electronic Structure and the Properties of Solids* (Freeman, San Franciso, 1980).
[22]D. van der Marel, J. Julianus, and G. A. Sawatzky, Phys. Rev. B **32**, 6331 (1985).
[23]A. Bosch, H. Feil, G. A. Sawatzky, and J. Julianus, J. Phys. F **14**, 2225 (1984).
[24]F. Patthey, B. Delley, W. D. Schneider, and Y. Baer, Phys. Rev. Lett. **55**, 1518 (1985).
[25]J. C. Slater, *Quantum Theory of Atomic Structure* (McGraw-Hill, New York, 1960), Pts. I and II.
[26]C. W. Nielson and G. F. Koster, *Spectroscopic Coefficients for P^n, d^n, and f^n Configurations* (MIT Press, Cambridge, Mass., 1963).
[27]These expressions follow from Ref. 30 by considering the case of a half-filled shell.
[28]J. F. Herbst, R. E. Watson, and J. W. Wilkins, Phys. Rev. B **13**, 1439 (1976).
[29]J. F. Herbst, D. N. Lowy, and R. E. Watson, Phys. Rev. B **6**, 1913 (1972).
[30]J. F. Herbst, R. E. Watson, and J. W. Wilkins, Phys. Rev. B **17**, 3089 (1978).
[31]J. F. Herbst and R. E. Watson, Phys. Rev. Lett. **34**, 1395 (1975).
[32]P. H. Dederichs, S. Blügel, R. Zeller, and M. Akai, Phys. Rev. Lett. **53**, 2512 (1984).
[33]J. Friedel, Nuovo Cimento **7**, 287 (1958).
[34]J. B. Mann, Los Alamos Scientific Laboratory Report No. LASL-3690, 1967 (unpublished).
[35]Y. Baer and G. Busch, J. Electron Spectrosc. Relat. Phenom. **5**, 611 (1974).
[36]M. Campagna, E. Bucher, G. K. Wertheim, and L. D. Longinotti, Phys. Rev. Lett. **33**, 165 (1974); **32**, 885 (1974).
[37]B. W. Veal, D. J. Lam, M. Diamond, and M. R. Hoekstra, Phys. Rev. B **15**, 2929 (1977).
[38]Y. Baer and J. Schoenes, Solid State Commun. **33**, 885 (1980).
[39]J. R. Naegele, L. Manes, J. C. Spirlet, and W. Müller, Phys. Rev. Lett. **52**, 1834 (1984).
[40]J. K. Lang, Y. Baer, and P. A. Cox, J. Phys. F **11**, 121 (1981).
[41]P. A. Cox, J. K. Lang, and Y. Baer, J. Phys. F **11**, 113 (1981).
[42]L. J. Nugent and K. L. van der Sluis, J. Opt. Soc. Am. **61**, 1112 (1971).
[43]Q. Günnarsson and K. Schönhammer, Phys. Rev. B **28**, 4315 (1983).
[44]L. Brewer, J. Opt. Soc. Am. **61**, 1101 (1971).
[45]P. T. Andrews and L. T. Brown, in *Physics of Transition Metals, 1980,* Inst. Phys. Conf. Ser. No. 55, edited by P. Rhodes (Institute of Physics, London, 1981), Chap. 3, p. 141; H. S. Reehal and P. T. Andrews, J. Phys. F **10**, 1631 (1980).
[46]D. van der Marel, G. A. Sawatzky, and F. U. Hillebrecht, Phys. Rev. Lett. **53**, 206 (1984); Phys. Rev. B **31**, 1936 (1985).
[47]E. Antonides and G. A. Sawatzky, Phys. Rev. B **15**, 1669 (1977).
[48]J. C. Fuggle, P. Bennet, F. U. Hillebrecht, A. Lenselink, and G. A. Sawatzky, Phys. Rev. Lett. **49**, 1787 (1982).
[49]H. W. Haak, Ph.D. thesis, University of Groningen, 1983; H. W. Haak, J. Zaanen, and G. A. Sawatzky (unpublished).
[50]N. Martensson, R. Nijholm, and B. Johansson, Phys. Rev. B **30**, 2245 (1984).
[51]C. E. Moore, *Atomic Energy Levels,* Natl. Bur. Stand. (U.S.) Circ. No. 467 (U.S. GPO, Washington, D.C., 1958). Pts. I–III.
[52]D. K. G. de Boer, C. Haas, and G. A. Sawatzky, J. Phys. F **14**, 2769 (1984).
[53]D. J. Lam and A. T. Aldred, in *The Actinides, Electronic Structure and Related Properties,* Ref. 8.
[54]H. M. Hill, in *Plutonium 1970,* edited by W. N. Miner (Metals Society of AIME, Metals Park, Ohio, 1970).
[55]B. Johansson, in *Valence Instabilities and Related Narrow-Band Phenomena,* Ref. 6, p. 435.
[56]B. Johansson, Phys. Rev. B **11**, 2740 (1975).
[57]B. Johansson, Philos. Mag. **30**, 469 (1974).
[58]J. Sticht and J. Kübler, Solid State Commun. **54**, 389 (1985);

A. M. Boring, R. C. Albers, G. R. Stewart, and D. D. Koeling, Phys. Rev. B **31**, 3251 (1985).
[59]B. T. Thole, G. van der Laan, J. C. Fuggle, G. A. Sawatzky, R. C. Karnatak, and J. M. Esteva, Phys. Rev. B **32**, 5107 (1985).
[60]G. R. Stewart, Rev. Mod. Phys. **56**, 755 (1984).
[61]T. Penney and F. Holzberg, Phys. Rev. Lett. **34**, 322 (1975).
[62]J. W. Allen and R. M. Martin, Phys. Rev. Lett. **49**, 1106 (1982).
[63]S. van Smaalen and C. Haas, Solid State Commun. **55**, 1027 (1985).
[64]J. E. Hirsch and D. J. Scalapino, Phys. Rev. B **32**, 5639 (1985).
[65]D. van der Marel and G. A. Sawatzky, Solid State Commun. **55**, 937 (1985).
[66]T. T. M. Palstra, A. A. Menovsky, J. van den Berg, A. J. Dirkmaat, P. H. Kes, G. J. Nieuwenhuys, and J. A. Mydosh, Phys. Rev. Lett. **55**, 2727 (1985).
[67]D. Riegel, J. Magn. Magn. Mater. **52**, 96 (1985).
[68]G. Gruner, Adv. Phys. **23**, 941 (1974).
[69]A. D. Caplin and C. Rizzuto, Phys. Rev. Lett. **21**, 746 (1968).
[70]P. Steiner, H. Hoechst, and S. Huefner, J. Phys. F **7**, L105 (1977).
[71]D. Riegel, H. J. Barth, L. Bürmann, H. Haas, and Ch. Stenzel, Phys. Rev. Lett. **57**, 388 (1986).